

Modeling Surround-aware Contrast Sensitivity

Shinyoung Yi[†] Daniel S. Jeon[†] Ana Serrano[‡]
Se-Yoon Jeong[§] Hui-Yong Kim[§] Diego Gutierrez[‡] Min H. Kim[†]
[†] KAIST [‡] Universidad de Zaragoza, I3A [§] ETRI

This supplemental document provides additional technical details and additional results from the main paper.

1. Experimental Setup

1.1. Display calibration

We found that the luminance of the center region, where the stimuli are shown, is affected by the luminance level of the surrounding area of the display, but not the other way around. We thus assume that the output luminance L^o of the stimuli follows $L^o = c(L^i, L_s^i)$, where L^i and L_s^i are the control signals of the intensity of the stimuli and the surrounding area, respectively, and c is a calibration function. The output luminance of the surrounding area L_s^o can be written as $L_s^o = c(L_s^i, L_s^i)$. Using a Specbos Jeti 1200 spectroradiometer, we measured the calibration functions c for all 25 different combinations of L^i and L_s^i , to accurately produce all our combinations of stimuli luminance and surrounding luminance. The calibration function we measured is shown in Figure 1.

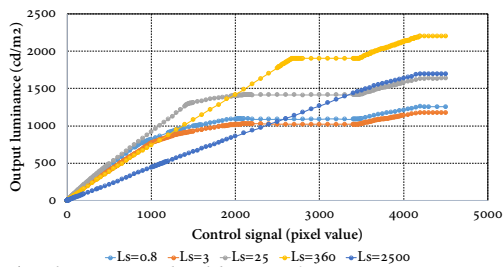


Figure 1: The measured calibration function. We measured L^o for fine levels of L^i and the five levels of L_s^i .

We measured this function at fine levels of L^i and the five levels of L_s^i . One notable effect is that the output luminance L^o does not increase even when the control signal L^i is changed in certain range. The cause is not clear, but it seems to be a limitation of HDR display technology which expresses extremely wide range of luminance.

After measuring these calibration functions, we regressed the five calibration function curves for each L_s^i as piecewise linear or cubic functions, and generated our experiment stimuli by applying the inverses of calibration functions to get intended luminance.

1.2. Stimuli

Each luminance value denotes the calibrated physical value, where the value of each pixel $I(x, y)$ can be expressed as:

$$I(x, y) = \begin{cases} L_s & \text{if } \text{deg}(x, y) > \frac{\pi}{2} \\ L(1 + C \cos(360^\circ \cdot u_{cpp}(x + \phi))) & \text{if } \text{deg}(x, y) \leq \frac{\pi}{2}, \text{ horizontal,} \\ L(1 + C \cos(360^\circ \cdot u_{cpp}(y + \phi))) & \text{if } \text{deg}(x, y) \leq \frac{\pi}{2}, \text{ vertical} \end{cases} \quad (1)$$

where $w = 1920$ and $h = 1080$ correspond to the pixel resolution, w_{mm} is the width of the screen in mm, $d = 1250$ mm is the distance of the observer, $u_{cpp} := u(X_o w_{mm}) / (2dw \tan(X_o/2))$ is the spatial frequency in cycles per pixel, ϕ denotes the offset of the sinusoidal pattern, and $\text{deg}(x, y) := \tan^{-1}((w_{mm}/dw) \max(|x - w/2|, |y - h/2|))$ denotes the angular position of pixel (x, y) . Here, C means a contrast ratio of the AC component to the DC component.

2. CSF Measurements

2.0.0.1. Horizontal vs. vertical CSF For our CSF measurement, there are virtually the same trend for horizontal and vertical CSFs (Figure 2). The geometric mean of the ratio of the horizontal CSF with respect to the vertical CSF (Figure 3) is about 1.16, so the vertical CSF is slightly higher than horizontal one on average, but the difference is not significant. Figure 4 shows the averaged CSF of the horizontal and vertical directions. Figure 5 compares our measured CSF with Barten's [Bar03] surround-aware CSF model.

2.1. Discussion

2.1.0.1. Stimuli Patterns Recent works on measuring CSF [MKRH11, LBLM14, WAK*20] use Gabor patch which smoothes the edge of the center area with sinusoidal pattern. The Gabor patch prevents the participants from detecting the edge of the center area rather than the sinusoidal pattern itself. The reason why we separated the center and surrounding areas without smoothing is that in our experiment smoothing the border between two areas yields rapid spatial change of luminance such as the case of $L = 0.56 \text{ cd/m}^2$ and $L_s = 1065.25 \text{ cd/m}^2$. This rapid luminance change at the intermediate area may effect on our surround-aware measurement. Thus, to make luminance of the surrounding area have a uniform luminance level, we did not use smoothing between

the two areas. Also, all of these works have measured the CSF at cases of $L = L_s$. For our experiment, at almost cases there are edges between the center area and the surrounding area since $L \neq L_s$ even if the center area has a zero contrast. Then detecting edges does not disturb detecting the sinusoidal pattern. Thus, even if we do not use Gabor patch, the effect will not be significant for surround-aware CSF.

2.1.0.2. Method of adjustment Recent works [RLN93, MKRH11, WAK*20] on measuring CSF use the method of constant stimuli instead of the method of adjustment, which we used. For the method of constant stimuli, participants respond multiple-alternative-choices (mAFCs), such as "vertical or horizontal" or "uniform or modulated pattern", for each levels of contrast values. It is known as yielding more accurate measurement for psychophysical experiment, but requires several times more time than the method of adjustment. Since we measure CSF for the four variables, D , u , L , and L_s , using the method of constant stimuli requires extremely long time. Thus, our experiment is done by the method of adjustment. To reduce error of measurement, we hired 13 participants. Compared to the psychophysical experiment often done with 6 or less participants [RC73, RLN93, MKRH11], 13 participants is sufficient to reduce the error.

3. CSF modeling

3.1. Barten's CSF model

Barten [Bar92] proposed a physical model of contrast sensitivity taking various parameters into account as following:

$$S_B^o(u, L) = \frac{M_{opt}(u)/k}{\sqrt{\frac{2}{T} \left(\frac{1}{X_o^2} + \frac{1}{X_{max}^2} + \frac{u^2}{N_{max}^2} \right) \left(\frac{1}{\eta p E} + \frac{\Phi_0}{1 - e^{-(u/u_0)^2}} \right)}}, \quad (2)$$

where $M_{opt}(u) = e^{-2\pi^2\sigma^2u^2}$ is the optical modulation transfer function, $\sigma = \sqrt{\sigma_0^2 + (C_a b d)^2}$ is the standard deviation of the line-spread function, $d = 5 - 3 \tanh(0.4 \log_{10} L)$ is the pupil diameter in mm, $E = \frac{\pi d^2}{4} L \left(1 - (d/9.7)^2 - (d/12.4)^4 \right)$ is the retinal illumination level in the Troland unit.

3.2. Modeling Relative Contrast Sensitivity

To model the relative contrast sensitivity $R(u, L^*)$, first we observed behavior of $R(u, L^*)$ at the log-log scale. r denotes the log-log scale function of R , so that

$$R(u, L^*) = 10^{r(u, l^*)}, \quad (3)$$

where $L^* = \frac{L_s}{L}$ and $l^* = \log_{10} L^*$. Then Figure 6, which is consisting of log-log scaled plots of the function R of L^* , shows the trend of the function r of l^* . We observed r as a function of l^* and found two trends. The first one is a concave trend, and the second one is that r decay more rapidly at $l^* \rightarrow \infty$ than $l^* \rightarrow -\infty$.

These trends we observed are related to the derivative $\frac{dr}{dl^*}$, so we constructed a model of $\frac{dr}{dl^*}$ first and then integrated it. We found

that functions of the form $-a(x + \sqrt{x^2 + d}) + b$ follows those trends. Here, d should be nonnegative. Appending an offset coefficient of x , we put $\frac{dr}{dl^*} = -a \left((l^* + c) + \sqrt{(l^* + c)^2 + d} \right) + b$. By integrating it and redefining some coefficients for simplicity, we get the following expression:

$$r(u, l^*; a, b, c, d) = -a(l^*)^2 + bl^* - a(l^* + c) \sqrt{(l^* + c)^2 + d} - ad \ln \left(\sqrt{(l^* + c) + d} + l^* + c \right) + a \left[c \sqrt{c^2 + d} + d \ln \left(\sqrt{c^2 + d} + c \right) \right] \quad (4)$$

where $l^* = \log_{10} L^*$. The constant of integration has been determined by the constraint $r(l^* = 0) = 0$.

Now we only have to model u dependency of r . Defining all parameters a , b , c , and d as functions of the spatial frequency u would provide the most accurate results, at the risk of overfitting our measurements. To avoid this overfitting, we first define

$$b' := b + 2ac, \quad (5)$$

which represents the partial derivative of r with respect to l^* so that $b' = \lim_{l^* \rightarrow -\infty} \frac{dr}{dl^*}(u, l^*)$. Parameters a , b' , c , and d can be modeled as functions of spatial frequency u , shown in the left part of Figure 7. We then model only b' and c as functions of u , and fit a and d as constants:

$$b'(u; q_1, q_2, q_3) = \frac{q_1}{1 + e^{q_2(\log_{10} u - q_3)}}, \quad (6)$$

$$c(u; p_1, p_2) = p_1 \log_{10} u + p_2,$$

where $q_{1,2,3}$ and $p_{1,2}$ are model parameters for b' and c , respectively. These fitting results of parameters b' and c are shown in the top-right and bottom-right plots in Figure 7, respectively.

The parametric function model for relative contrast sensitivity should have the following constraints to maintain its trend and to be defined on any real numbers:

$$a \geq 0 \text{ and } d \geq 0. \quad (7)$$

Note that as long as these constraints hold the trends of the model r , such as concavity and asymptotic behavior, does not change so that we can use this model to fit to our data. Figures 6 is the complete version of Figure 4 in the main paper.

As shown in Figure 6, our relative sensitivity $R(u, L^*)$ as a function of the ratio between surround luminance L_s and stimulus luminance L . From left to right (increasing spatial frequency u), it can be seen how the slope flattens for negative values of L^* . The plots on the bottom line shows our *practical* relative sensitivity $R_p(L^*)$, which does not depend on u . However, from regression, we obtained a negative $b' = -0.020$ value for the highest level of $u=20.16$ cpd., which yields a property that $r(x)$ has negative slopes at $x < 0$ ($L^* < 1$). This property highly contradicts the *crispening effect* [Whi86] that the luminance resolving power of human eyes is maximized when the adaptation luminance level is close to the target luminance. If b' is negative, our CSF formulae becomes the infinite sensitivity when L_s is zero, which does not make a sense. Also, the estimated negative value of $b'(u = 20.16 \text{ cpd.}) = -0.020$

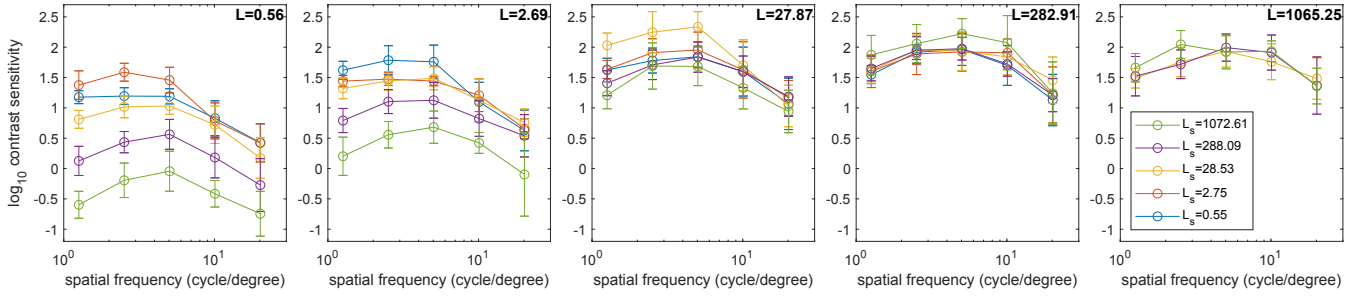


Figure 2: Our surrounded CSF measurement in the horizontal direction. The length of one side of the error bar indicates one standard deviation of participants' responses.

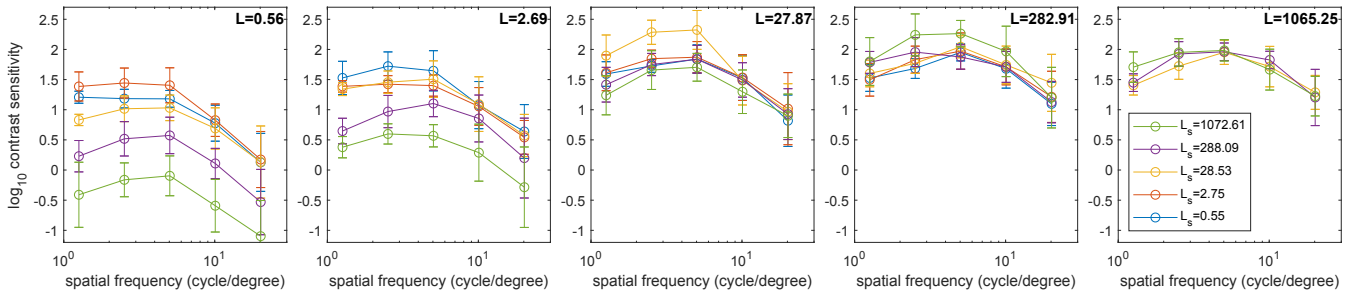


Figure 3: Our surrounded CSF measurement in the vertical direction.

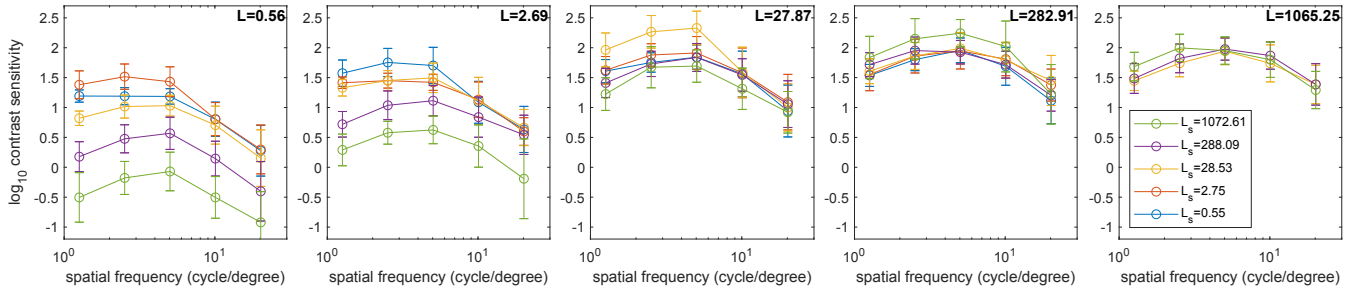


Figure 4: Our surrounded CSF measurement averaged in both horizontal and vertical directions.

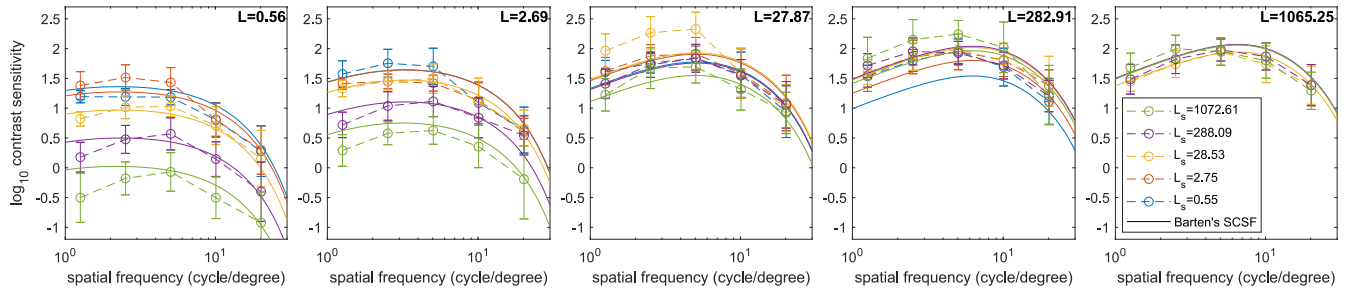


Figure 5: Our surrounded CSF measurements compared with Barten's [Bar03] model.

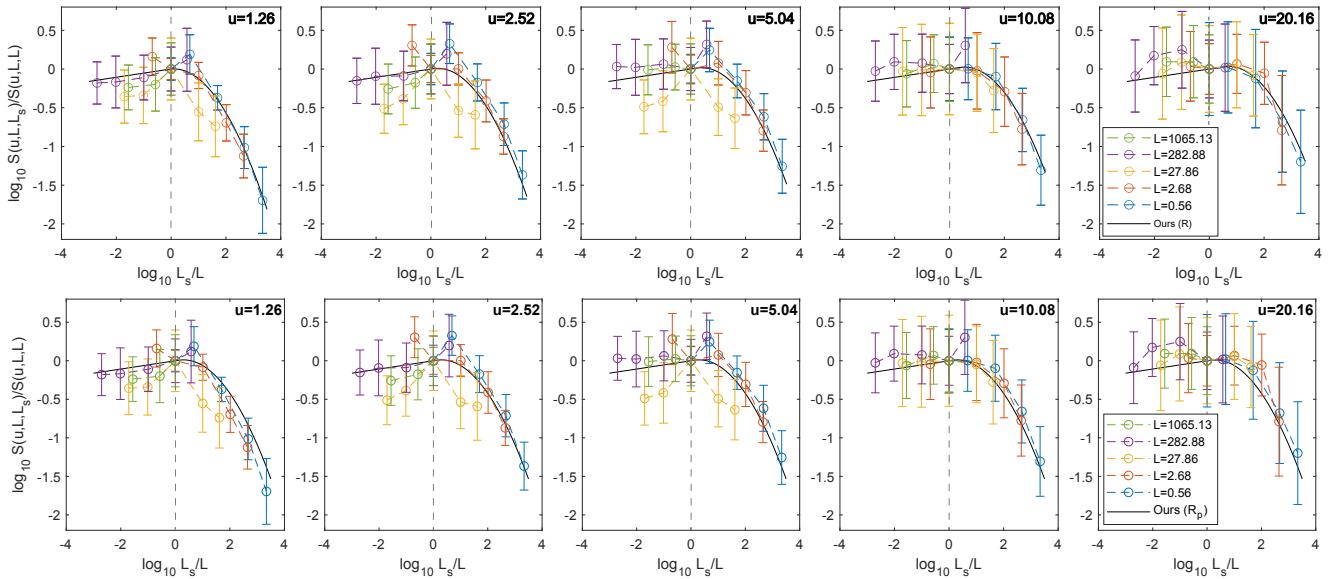


Figure 6: Comparison of our regressed functions. (Top) Modeling the relative CSF about L_s as a function R of spatial frequency u and the luminance ratio L^* . (Bottom) Modeling the relative CSF about L_s as a function R_p of the luminance ratio L^* .

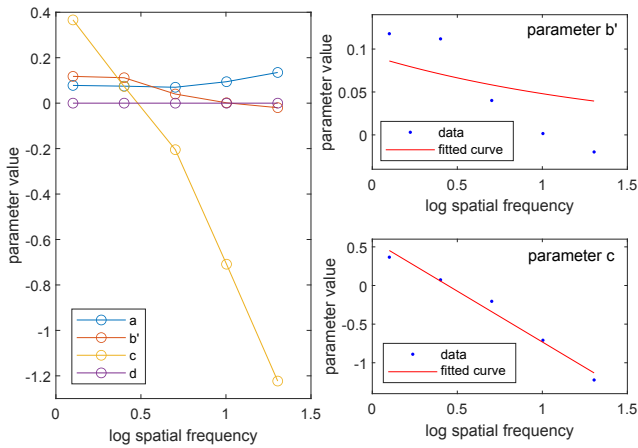


Figure 7: Parameters a , b' , c , and d , which determines the model r described in Equation (4). b' is defined in Equation (5). The model r is fitted to the measured relative sensitivity data for each spatial frequency u separately. Then parameter values a , b' , c , and d can be obtained for each u .

is not significant since its 95% confidence interval $(-0.062, 0.022)$ still contains a positive region, so we have decided that the negative value of b' ($u = 20.16$ cpd.) $= -0.020$ is an overestimation. By these two reasons, $b' < 0$ contradicts to the crispening effect and the estimated negative b' value is not significant, we have decided to model $b'(u)$ as a function which only has positive value.

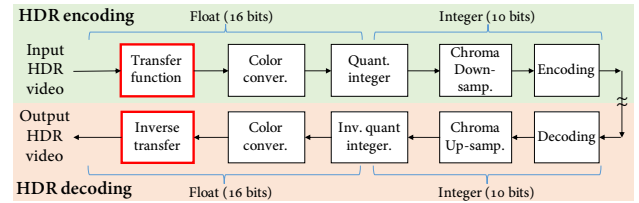


Figure 8: (a) Standard HDR video coding pipeline specified in [ITU17].

4. HDR image/video applications

4.1. HDR video compression

The entire pipeline of video compression standardized by [ITU17] is shown in Figure 8. Among this entire pipeline, we derived a transfer function from our practical CSF model. Following the process proposed by Miller et al. [MND13], we first remove u dependency of CSF to obtain a function only depend on luminance by taking the maximum of CSF about u , i.e., $S(L) := \max_u S(u, L)$. Second, we define the distance between two slightly different luminance values L_1 and L_2 as $d(L_1, L_2) := |L_1 - L_2| / (L_1 + L_2) \cdot S((L_1 + L_2) / 2)$, which yields $d(L_1, L_2) = 1$ whenever L_1 and L_2 have just noticeable difference. Lastly, our CSF-based transfer function F is designed to approximately satisfy $|F(L + \Delta L) - F(L)| \propto d(L + \Delta L, L)$ for any luminance value L and very small luminance value ΔL . In summary, one can define a perceptual distance between the luminance values from the CSF and the CSF-based transfer function is defined as a function that maps luminance values into a perceptually uniform space, given a surround luminance level. We compute transfer functions for each surround luminance level, yielding an adaptive transfer function.

References

- [Bar92] BARTEN P. G.: Physical model for the contrast sensitivity of the human eye. In *Human Vision, Visual Processing, and Digital Display III* (1992), vol. 1666, International Society for Optics and Photonics, pp. 57–72.
- [Bar03] BARTEN P. G.: Formula for the contrast sensitivity of the human eye. In *Image Quality and System Performance* (2003), vol. 5294, International Society for Optics and Photonics, pp. 231–238.
- [ITU17] ITU-R: Itu recommendation sector, bt. 2100-1: Image parameter values for high dynamic range television for use in production and international program exchange.
- [LBLM14] LEE T.-H., BAEK J., LU Z.-L., MATHER M.: How arousal modulates the visual contrast sensitivity function. *Emotion* 14, 5 (2014), 978.
- [MKRH11] MANTIUK R., KIM K. J., REMPEL A. G., HEIDRICH W.: Hdr-vdp-2: A calibrated visual metric for visibility and quality predictions in all luminance conditions. *ACM Transactions on graphics (TOG)* 30, 4 (2011), 1–14.
- [MND13] MILLER S., NEZAMABADI M., DALY S.: Perceptual signal coding for more efficient usage of bit codes. *SMPTE Motion Imaging Journal* 122, 4 (2013), 52–59.
- [RC73] ROGERS J. G., CAREL W. L.: *Development of design criteria for sensor displays*. Tech. rep., HUGHES AIRCRAFT CO CULVER CITY CA DISPLAY SYSTEMS DEPT, 1973.
- [RLN93] ROVAMO J., LUNTINEN O., NÄSÄNEN R.: Modelling the dependence of contrast sensitivity on grating area and spatial frequency. *Vision Research* 33, 18 (1993), 2773–2788.
- [WAK*20] WUERGER S., ASHRAF M., KIM M., MARTINOVIC J., PÉREZ-ORTIZ M., MANTIUK R. K.: Spatio-chromatic contrast sensitivity under mesopic and photopic light levels. *Journal of Vision* 20, 4 (2020), 23–23.
- [Whi86] WHITTLE P.: Increments and decrements: luminance discrimination. *Vision research* 26, 10 (1986), 1677–1691.